Mathematical Morphology and Eikonal Equations on Graphs for Nonlocal Image and Data Processing

Vinh Thong Ta, Abderrahim Elmoataz, Olivier Lézoray

Mathematical Morphology and Eikonal Equations on Graphs for Nonlocal Image and Data Processing

Vinh-Thong Ta, Abderrahim Elmoataz and Olivier Lézoray

Abstract

Mathematical morphology (MM) offers a wide range of operators to address various image processing problems. These operators can be defined in terms of algebraic (discrete) sets or as partial differential equations (PDEs). In this paper, we introduce a novel formulation of MM formalized as a framework of partial difference equations (PdEs) over weighted graphs of arbitrary topology. Then, we present and analyze a new family of morphological operators defined on weighted graphs. The proposed framework recovers local algebraic and PDEs-based formulations of MM. It also introduces nonlocal configurations for morphological image processing and extends PDEs-based methods to process any discrete data that can be described by a graph such as high dimensional data defined on irregular domains. Moreover, based on same ideas, we propose an adaptation of the eikonal equation on weighted graphs. Our formulation of the eikonal leads to novel applications of this equation such as nonlocal image segmentation and weighted distances or data clustering.

Index Terms

Mathematical morphology, partial difference equations (PdEs), weighted graphs, arbitrary discrete data sets, eikonal equation, nonlocal image segmentation, data clustering.

I. Introduction

Mathematical morphology (MM) is a popular nonlinear approach for image processing that has found numerous applications including shape and texture analysis, biomedical image processing, document recognition or multi-resolution techniques.

First developed by Matheron and Serra in [1], [2], MM relies on a fundamental structure, the complete lattice L [3]. A complete lattice L is a non-empty set equipped with an ordering relation, such that every non-empty subset K of L has a lower bound and an upper bound. In this context, images are modeled by functions mapping their domain space

The authors are with the Université de Caen Basse-Normandie, ENSICAEN in the GREYC Laboratory, Image Team, 6 Boulevard Maréchal Juin, F-14050 Caen Cedex, France.

Emails: vinhthong.ta@unicaen.fr, abderrahim.elmoataz-billah@unicaen.fr, olivier.lezoray@unicaen.fr

Phone: +33(0)231452706, Fax: +33(0)231452698

Ω, into a complete lattice L. With the acceptance of complete lattice theory, it is possible to define morphological operators for any type of image data once a proper ordering is established. Within this model, morphological operators are represented as mappings between complete lattices in combination with matching patterns called structuring elements that are subsets of Ω. In particular, the two fundamental operators in MM are dilation and erosion that form the basis of many other morphological processes such as opening/closing, reconstruction or levelings [4], [5]. As a consequence, the implementation of such morphological operators is usually performed within an algebraic (discrete) setting.

An alternative to the algebraic formulation of MM operators relies on nonlinear partial difference equations (PDEs). Following a PDEs-based formulation of low-level vision, some works have casted algebraic MM into the axiomatic framework of scale-space theory. This effort has led to derive continuous elementary morphological operators that model multiscale morphological scale space [6]–[8]. This PDEs framework has several advantages with respect to the standard algebraic formulation mentioned above while providing a better mathematical modeling and connection with physics. First, it offers excellent results for non-digitally scalable structuring elements whose shapes cannot be correctly represented on a discrete grid. Second, it allows sub-pixel accuracy and third, it can be adaptative by introducing a local speed evolution term [9]. To be applicable to images, PDEs are discretized with finite difference equations and numerical schemes based on curve evolution ideas [10]–[12] have been developed to approximate their solution.

Whatever the chosen formulation (algebraic or PDEs), if MM is well defined for binary and gray scale images, there exists no general extension for the processing of multivariate unorganized data sets. With the algebraic formulation, performing basic morphological operations on multivariate data requires a complete lattice. However, there is no natural ordering on vectors. Several orderings have been reported in literature (see [13] for a complete review) to consider that problem but they are reduced to specific types of images (color [14] or tensor [15] images). Moreover, the processing of arbitrary unorganized data is difficult with algebraic MM and very few works consider that issue. Algebraic MM has been defined for graphs [16], [17], but only for particular graphs (for instance on binary graphs or on minimum spanning trees). It has also been applied to data and cluster analysis [18] with the drawback of requiring regular discrete grids. With the PDEs MM formulation, one also has the same drawback for unorganized data because the spatial discretization is difficult. Regarding all these considerations, there is actually no satisfying formulation of MM for the processing of multivariate unorganized data. The algebraic formulation has drawbacks for multivariate data and the PDEs formulation has drawbacks for unorganized data.

In addition, whatever the formulation (algebraic or PDEs), both only consider local interactions on the data while nonlocal schemes have recently received a lot of attention. Nonlocal schemes enable to better capture the complex structure of the data and have shown their effectiveness for the processing of images, manifolds, meshes and arbitrary data processing [19]–[22]. Unfortunately, the use of nonlocal interactions has never been investigated in MM whatever the formulation.

Inspired by previous works of [22], [23] that define a discrete analogue of continuous regularization over graphs, we propose to consider a discrete version of continuous MM over weighted graphs that naturally enables nonlocal processing of any multivariate data living on any domain. Our main contributions are detailed in the sequel.

Contributions. In this paper, we propose to extend the PDEs-based MM operators to a discrete scheme by considering partial difference equations (PdEs) over weighted graphs of arbitrary topology [24], [25].

To this aim, nonlocal discrete derivatives on graphs are introduced to transcribe MM processing based on the continuous PDEs to PdEs over graphs. This comes to define a third formulation for MM based on partial difference equations. Our approach of MM operations has several advantages. First, any discrete domain modeled by a graph can be considered without any spatial discretization as required by the PDEs formulation. Second, any multivariate data can be processed without requiring the definition of a complete lattice as required by the algebraic formulation. Therefore, the proposed PdEs formulation tackles the above-mentioned drawbacks of classical formulations of MM. These points enable new insights in data mining by morphological processing of multivariate unorganized data. Third, our formulation has the advantage of naturally enabling local and nonlocal interactions modeling within a same formulation [26]. This point allows to introduce adaptation in image processing (e.g. to preserve some geometrical and repetitive structures in images). Moreover, we show that our formulation recovers well known MM implementations schemes such as Osher-Sethian discretization scheme [10] and algebraic formulations on graphs. Finally, another advantage of working with graphs in the context of image processing is that higher abstraction elements than image pixels such as image regions can be used [24], [25]. This latter approach allows faster algorithms by reducing the amount of data to analyze.

In addition to fundamental MM operations, we focus on the one hand on general classes of morphological filters, the levelings, that include reconstruction openings and closings [27] and propose a discrete analogue of such filters on graphs [28]. On the other hand, we also propose an adaptation of the continuous eikonal PDE by considering the latter on weighted graphs of arbitrary structure. As it will be discussed, a same framework can be derived for computing the solution of the eikonal equation on graphs that enables novel applications of this equation such as local and nonlocal image segmentation and weighted distances or data clustering [29].

The paper is structured as follows. Section II recalls definitions of algebraic and PDEs formulations of morphological erosion and dilation. Section III provides basic notions on weighted graphs and key points for their construction (topology and weights). Section IV presents new operators on graphs that will be the basis for our MM formulation. Section V presents our MM formulation by partial difference equations over graphs. This Section defines basic dilation and erosion as well as levelings over graphs and our adaptation of the eikonal equation. Section VI and Section VII show experiments of local and nonlocal processing and segmentation of images and unorganized high dimensional discrete data sets. Section VIII concludes.

II. Morphological dilation and erosion

With a functional terminology [30], morphological dilation $\delta:\mathbb{R}^n \to \mathbb{R}^n$ and erosion $\varepsilon:\mathbb{R}^n \to \mathbb{R}^n$ of a function $f^0:\mathbb{R}^n \to \mathbb{R}$ are usually formulated by

$$\begin{aligned} &\delta_z(f^0)(x) = \sup\{f^0(x-y) + z(y) : y \in B\} \text{ and} \\ &\varepsilon_z(f^0)(x) = \inf\{f^0(x+y) - z(y) : y \in B\} \end{aligned} ,$$

where $x{\in}\mathbb{R}^n$ and $z{:}B{\to}\mathbb{R}$ is a function or a multi-level structuring element with finite support set $B{=}\{y : z(y){>}{-}\infty\}$.

In practice, a useful class of functions z consists in flat structuring functions i.e. $z(y){=}0$ if $y{\in}B$ and $z(y){=}{-}\infty$ otherwise. If B is a compact convex symmetric set, then definitions of dilation and erosion become

$$\begin{aligned}&\delta_B(f^0)(x){=}\sup\{f^0(x{+}y) : y{\in}B\} \text{ and}\\&\varepsilon_B(f^0)(x){=}\inf\{f^0(x{+}y) : y{\in}B\}\end{aligned}\;.$$

By using structuring sets $B{=}\{x : \|x\|_p{\leq}1\}$, the general PDEs generating these *flat* dilations and erosions [31] are as follows:

$$\frac{\partial\delta(f)}{\partial t}{=}\partial_t f{=}{+}\|\nabla f\|_p \text{ and } \frac{\partial\varepsilon(f)}{\partial t}{=}\partial_t f{=}{-}\|\nabla f\|_p \tag{1}$$

where f is a modified version of f^0, ∇ is the gradient operator, $\|.\|_p$ corresponds to the $\mathcal{L}_p$-norm, and one has the initial condition $\partial_{t=0}f{=}f^0$. With different values of p, one obtains different structuring elements: a rhombus for $p{=}\infty$, a disc with $p{=}2$ and a square with $p{=}1$ [31].

In this paper, we only consider the case of flat morphology.

III. Weighted graphs

The core idea of our approach is to define morphological operators on weighted graphs of arbitrary structure. Hence, in this Section, basics notions on weighted graphs are recalled, and key points on graph construction are detailed (distance between vertices, graph topology, and edges weights). All the following definitions and notations are used throughout this paper.

A. Basic notions

We consider the general situation where any discrete domain can be viewed as a weighted graph. Let $G{=}(V,E,w)$ be a *weighted graph* composed of a finite set of *vertices* V and a finite set of *weighted edges* $E{\subseteq}V{\times}V$. An edge $(u,v){\in}E$ connects two *adjacent* or *neighbor* vertices u and v of V. The set of neighbors of a vertex u is denoted by $N(u){=}\{v{\in}V{\setminus}\{u\} : (u,v){\in}E\}$. The weight $w{:}V{\times}V{\to}\mathbb{R}^+$ of an edge $(u,v){\in}E$ can be defined by $w(u,v)$, if $(u,v){\in}E$ and $w(u,v){=}0$, otherwise.

In this work, graphs are assumed to be simple, connected and undirected, implying that the weight function w is symmetric $w(u,v){=}w(v,u)$ for all $(u,v){\in}E$. More details on these notions can be found in [32]. For the sake of simplicity, $w(u,v)$ will be denoted by w_{uv} and notation $v{\sim}u$ will mean that vertices u and v are adjacent.

Let $f{:}V{\to}\mathbb{R}$ be a discrete real-valued function that assigns a real value $f(u)$ to each vertex $u{\in}V$. We denote by $\mathcal{H}(V)$ the Hilbert space of such functions defined on the vertices of G. Similarly, let $\mathcal{H}(E)$ be the Hilbert space of functions that assign a real value to each edge of E. These two spaces are endowed with the usual inner products [22].

B. Graph construction

Any discrete domain can be modeled by a weighted graph where each data point is represented by a vertex $u{\in}V$. This domain can represent *unorganized* or *organized* data where functions defined on $\mathcal{H}(V)$ correspond to the data to process.

1) Unorganized data: In this general case, the unorganized set of points $V{\subset}\mathbb{R}^n$ can be seen as a function $f^0{:}V{\subset}\mathbb{R}^n{\to}\mathbb{R}^n$. Then, defining the set of edges consists in modeling the neighborhood of each vertex that is based on similarity relationships between the feature vectors of the data set. This similarity depends on a pairwise distance measure $\mu{:}V{\times}V{\to}\mathbb{R}^+$. A typical choice of μ for unorganized data is the Euclidean distance. Graph construction is application dependent and no general rules can be given. However, there exists several methods to construct a neighborhood graph. Typical graph structures can be quoted: the τ-neighborhood graph, the k-nearest neighbors graph, the complete graph, the minimum spanning tree or the relative neighborhood graph (see [33] for a survey on proximity and neighborhood graphs).

In this paper, we focus on two classes of graphs: a modified version of k-nearest neighbors graphs and τ-neighborhood graphs.

The k-nearest neighbors graph, noted k-NNG$=(V,E,w)$ is a weighted graph where each vertex $u{\in}V$ is connected to its k nearest neighbors ($NN_k(u){\in}V\setminus\{u\}$) that have the smallest distance measure towards u according to function μ. Since this graph is directed, a modified version of this graph is used to make it undirected, i.e. $E=\{(u,v): u{\in}NN_k(v) \text{ or } v{\in}NN_k(u)\}$ for $u,v{\in}V$.

The τ-neighborhood graph, noted $G_\tau=(V,E,w)$ is a weighted graph where the τ-neighborhood N_τ for a given vertex $u{\in}V$ is defined as $N_\tau(u){=}\{v{\in}V\setminus\{u\}:\mu(u,v){\leq}\tau\}$ with $\tau{>}0$ is a threshold parameter.

2) Organized data: Typical cases of organized data are signals or images (2D or 3D). Such data can be seen as functions $f^0{:}V{\subset}\mathbb{Z}^m{\to}\mathbb{R}^n$ with $m{=}1,2$ or 3 corresponding to the above mentioned cases. Then, the distance μ used to construct the graph corresponds to a distance between spatial coordinates associated to vertices V. Several distances can be considered among those, we can quote the city-block or the Chebyshev distances.

For a 2D image, the city-block and the Chebyshev distances between vertices u and v associated with their spatial coordinates (x_i,y_i) and (x_j,y_j) are defined as $\mu(u,v)=|x_i{-}x_j|{+}|y_i{-}y_j|$ and $\mu(u,v)=\max(|x_i{-}x_j|,|y_i{-}y_j|)$, respectively. With these distances and a τ-neighborhood graph, one can recover the usual adjacency graphs used in 2D image processing where each vertex corresponds to an image pixel. A 4-adjacency grid graph (denoted as G_0 in the rest of this paper) is obtained with a city-block distance and $\tau{\leq}1$. A 8-adjacency grid graph (further denoted as G_1) is obtained with a Chebyshev distance and $\tau{\leq}1$. More generally, $((2s{+}1)^2{-}1)$–adjacency graphs are obtained with a Chebyshev distance with $\tau{\leq}s$ and $s{\geq}1$. This corresponds to add edges between the central pixel of a square window of size $(2s{+}1){\times}(2s{+}1)$ and the other pixels within the window. Similar remarks apply for the construction of graphs on 3D images where vertices are associated to voxels.

One can also consider the case of Region Adjacency Graphs (RAG) where each vertex corresponds to one region. The set of edges is obtained with an adjacency distance: $\mu(u,v)=1$ if u and v are adjacent and $\mu(u,v)=\infty$ otherwise, together with a τ-neighborhood graph ($\tau{=}1$): this corresponds to the Delaunay graph of an image partition.

Finally, we can mention the cases of polygonal curves or surfaces that have natural graph representations where vertex correspond to mesh vertices and edges are mesh edges.

C. Graph weights

For a given function $f^0{\in}\mathcal{H}(V)$, similarity relationship between data can be incorporated within edges weights according to a measure of similarity $g{:}E{\to}\mathbb{R}^+$ and with $w(u,v){=}g(u,v)$.

Computing distances between vertices consists in comparing their features that generally depend on the initial function f^0. To this aim, each vertex $u{\in}V$ is assigned with a feature vector $F(f^0,u){\in}\mathbb{R}^m$. Then, the following weight functions can be considered. For a given edge $(u,v){\in}E$ and a distance measure $\rho{:}V{\times}V{\to}\mathbb{R}^+$ associated to F, we can have:

$$g_0(u,v){=}1 \text{ (unweighted case) },$$

$$g_1(u,v){=}\exp(-\rho(F(f^0,u),F(f^0,v))^2/\sigma^2) \text{ with } \sigma{>}0 \ ,$$

$$g_2(u,v){=}(\rho(F(f^0,u),F(f^0,v))+\epsilon)^{-1} \text{ with } \epsilon{>}0, \epsilon{\to}0 \ .$$

Usually, the distance function ρ is the Euclidean distance function. Several choices can be considered for the expression of F depending on the features to preserve. The simplest one is $F(f^0,u){=}f^0(u)$.

In the context of image processing, an important feature vector F is provided by images patches i.e. $F(f^0,u) = F_\tau(f^0,u) = \{f^0(v) : v{\in}N_\tau(u) \cup \{u\}\}$. In the case of a grayscale image $F_\tau(f^0,.)$ is a vector of size $(2\tau{+}1)^2$ corresponding to the values of f^0 in a square window of size $(2\tau{+}1){\times}(2\tau{+}1)$ centered at vertex u (a pixel). Color images can be handled using features of dimension $3{\times}(2\tau{+}1)^2$. Then, the resultant weight function directly incorporates local or nonlocal features [26]. This feature vector has been proposed in the context of texture synthesis [34], and further used in the context of image processing [19], [20].

IV. OPERATORS ON WEIGHTED GRAPHS

In this Section, we define operators on weighted graphs that constitute the basis of our morphological framework.

A. Weighted morphological difference operators

All the basic operators considered in this paper are defined from the difference operator or the discrete derivative. There exists several definitions of these operators on graphs (see for instance [35]). In this work, we consider a definition that allows the expressions of discrete weighted gradient on graphs.

The *weighted difference operator* [23] $d_w{:}\mathcal{H}(V){\to}\mathcal{H}(E)$ of a function $f{\in}\mathcal{H}(V)$ is the vector of all weighted discrete derivatives:

$$d_w f{=}\big((d_w f)(u,v)\big)_{(u,v)\in E} \ ,$$

where for all $(u,v){\in}E$

$$(d_w f)(u,v){=}w_{uv}^{1/2}\big(f(v){-}f(u)\big) \ , \tag{2}$$

and

$$\partial_v f(u)=(d_w f)(u,v) \tag{3}$$

is the *discrete partial derivative* of f. This definition has the following properties for a function defined in a Euclidean space: $\partial_v f(u)=-\partial_u f(v)$, $\partial_u f(u)=0$ and if $f(u)=f(v)$ then $\partial_v f(u)=0$.

Based on the difference operator (2), we define two new *weighted morphological directional difference operators*. The weighted morphological *external* and *internal* difference operator are respectively:

$$\begin{aligned}
&(d_w^+ f)(u,v)=w_{uv}^{1/2}\big(\max\big(f(u),f(v)\big)-f(u)\big) \text{ and}\\
&(d_w^- f)(u,v)=w_{uv}^{1/2}\big(f(u)-\min\big(f(u),f(v)\big)\big) \ ,
\end{aligned} \tag{4}$$

with the following properties

$$\begin{aligned}
&(d_w^+ f)(u,v)=\max\big(0,(d_w f)(u,v)\big),\\
&(d_w^- f)(u,v)=-\min\big(0,(d_w f)(u,v)\big) \text{ and}\\
&(d_w^- f)(u,v)=(d_w^+ f)(v,u) \ .
\end{aligned}$$

Indeed, for the directional external difference operator and since $\max(a,b)-a=\max(0,a-b)$, we have

$$\begin{aligned}
(d_w^+ f)(u,v) &= w_{uv}^{1/2}\big(\max\big(f(u),f(v)\big)-f(u)\big)\\
&= w_{uv}^{1/2}\max\big(0,f(v)-f(u)\big)\\
&= \max\big(0,(d_w f)(u,v)\big) \ .
\end{aligned}$$

Similarly, for the internal difference operator, since $a-\min(a,b)=-\min(0,b-a)$, we have

$$\begin{aligned}
(d_w^- f)(u,v) &= w_{uv}^{1/2}\big(f(u)-\min\big(f(u),f(v)\big)\big)\\
&= -w_{uv}^{1/2}\min\big(0,f(v)-f(u)\big)\\
&= -\min\big(0,(d_w f)(u,v)\big) \ .
\end{aligned}$$

Finally, since $\max\big(0,a-b\big)=-\min\big(0,b-a\big)$ we obtain $(d_w^- f)(u,v)=(d_w^+ f)(v,u)$.

The two proposed weighted morphological directional difference operators (4) recover classical directional difference operators on unweighted graphs ($w=g_0=1$) and extend them to weighted graphs that enables more adaptation in the difference computation.

Based on definition (3), the corresponding external and internal partial derivatives are

$$\partial_v^+ f(u)=(d_w^+ f)(u,v) \text{ and } \partial_v^- f(u)=(d_w^- f)(u,v) \ . \tag{5}$$

B. Weighted morphological gradients and norms

The *weighted gradient* of a function $f\in\mathcal{H}(V)$ at vertex u is the vector of all edge directional derivatives

$$(\nabla_w f)(u)=\big(\partial_v f(u)\big)_{(u,v)\in E} \ . \tag{6}$$

Following this definition, we introduce two *new weighted morphological (internal and external) gradients* based on the partial derivatives (5) such as

$$\begin{aligned} &(\nabla_w^+ f)(u) = \big(\partial_v^+ f(u)\big)_{(u,v)\in E} \text{ and} \\ &(\nabla_w^- f)(u) = \big(\partial_v^- f(u)\big)_{(u,v)\in E} \ . \end{aligned} \tag{7}$$

The external gradient of a function is a directional difference operator defined as the difference between an extensive operator and the function (a typical one being the $\max$). Similarly, the internal gradient uses an anti-extensive (the $\min$) operator [36].

In the sequel, we use the $\mathcal{L}_p$-norm of gradients (7) for a given vertex $u \in V$, we have

$$\begin{aligned} \|(\nabla_w^+ f)(u)\|_p &= \Big[\sum_{v\sim u} w_{uv}^{p/2} \big|\max\big(0, f(v) - f(u)\big)\big|^p\Big]^{1/p} \text{ and} \\ \|(\nabla_w^- f)(u)\|_p &= \Big[\sum_{v\sim u} w_{uv}^{p/2} \big|\min\big(0, f(v) - f(u)\big)\big|^p\Big]^{1/p} \ ; \end{aligned} \tag{8}$$

and for the $\mathcal{L}_\infty$-norm, we have

$$\begin{aligned} \|(\nabla_w^+ f)(u)\|_\infty &= \max_{v\sim u}\Big(w_{uv}^{1/2} \big|\max\big(0, f(v) - f(u)\big)\big|\Big) \text{ and} \\ \|(\nabla_w^- f)(u)\|_\infty &= \max_{v\sim u}\Big(w_{uv}^{1/2} \big|\min\big(0, f(v) - f(u)\big)\big|\Big) \ . \end{aligned} \tag{9}$$

Same expressions can be obtained for the general weighted gradient (6).

One can note that general definitions presented in this Section are defined on graphs of arbitrary topology. Hence, they can be used to process any discrete regular or irregular data sets that can be represented by a weighted graph. Moreover, local and nonlocal settings are directly handled in these definitions and both are expressed by the graph topology in terms of neighborhood connectivity [22].

C. Relations with algebraic morphological operators

The previously defined external and internal gradients operate on any graph structure. In the sequel, we show that in the particular case of an unweighted ($w = g_0$) graph and with $p = \infty$, our gradient formulations recover algebraic morphological operators where the structuring element is provided by the graph neighborhood i.e. $B = N(u)$ for all $u \in V$.

The $\mathcal{L}_\infty$-norms (9) of the proposed external and internal gradients ∇_w^+ and ∇_w^- recover the classical definition of algebraic morphological external ($\delta(f)(u) - f(u)$) and internal ($f(u) - \varepsilon(f)(u)$) gradients. Indeed, for the external gradient

$$\begin{aligned} \|(\nabla_w^+ f)(u)\|_\infty &= \max_{v\sim u}\big(\max\big(0, f(v) - f(u)\big)\big) \\ &= \max_{v\sim u}\big(\max\big(f(u), f(v)\big) - f(u)\big) \\ &= \max_{v\sim u}\big(f(u), f(v)\big) - f(u) \\ &= \delta(f)(u) - f(u) \ , \end{aligned}$$

and similarly for the internal one

$$\begin{aligned}\|(\nabla_w^- f)(u)\|_\infty &= \max_{v\sim u}\big(|\min\big(0, f(v)-f(u)\big)|\big)\\ &= \max_{v\sim u}\big(\max\big(0, f(u)-f(v)\big)\big)\\ &= \max_{v\sim u}\Big(0, f(u)-f(v)\Big)\\ &= -\min_{v\sim u}\Big(0, f(v)-f(u)\Big)\\ &= f(u)-\min_{v\sim u}\Big(f(u), f(v)\Big)\\ &= f(u)-\epsilon(f)(u)\ \ .\end{aligned}$$

With these latter relations, we immediately recover the algebraic classical morphological gradient and Laplace operators:

$$\|(\nabla_w^+ f)(u)\|_\infty + \|(\nabla_w^- f)(u)\|_\infty = \delta(f)(u) - \varepsilon(f)(u) \text{ and}$$

$$\|(\nabla_w^+ f)(u)\|_\infty - \|(\nabla_w^- f)(u)\|_\infty = \delta(f)(u) + \varepsilon(f)(u) - 2f(u)\ \ .$$

Finally, our formulation recovers classical morphological gradient and Laplace operators and extend them to weighted graphs that define new families of local and nonlocal weighted morphological gradients and Laplace operators.

D. Graph boundary sets and relations with weighted morphological gradients

Let $\mathcal{A}$ be a set of connected vertices with $\mathcal{A}\subset V$ such that for all $u\in\mathcal{A}$, there exists a vertex $v\in\mathcal{A}$ with $(u,v)\in E$. We denote by $\partial^+\mathcal{A}$ and $\partial^-\mathcal{A}$, the *external* and *internal* boundary sets of $\mathcal{A}$, respectively. For a given vertex $u\in V$:

$$\begin{aligned}\partial^+\mathcal{A} &= \{u\in\mathcal{A}^c : \exists v\in\mathcal{A} \text{ with } (u,v)\in E\} \text{ and}\\ \partial^-\mathcal{A} &= \{u\in\mathcal{A} : \exists v\in\mathcal{A}^c \text{ with } (u,v)\in E\}\ \ ,\end{aligned} \tag{10}$$

where $\mathcal{A}^c = V\setminus\mathcal{A}$ is the complement of $\mathcal{A}$.

Figure 1 illustrates these notions on two different graph structures: a 4-adjacency grid graph and an arbitrary graph. One can remark that the boundary of V cannot be defined directly from the previous definitions, we assume it is known.

Intuitively from definitions (10), dilation over $\mathcal{A}$ can be interpreted as a growth process that adds vertices from $\partial^+\mathcal{A}$ to $\mathcal{A}$. By duality, erosion over $\mathcal{A}$ can be interpreted as a contraction process that removes vertices from $\partial^-\mathcal{A}$.

The following propositions show the relation between graph boundary sets and the weighted discrete morphological gradient norms (8) of the level set function of f at vertex $u\in V$. The decomposition of f into its level sets is denoted $f^l = \chi(f-l)$ where χ is the Heaviside function (a step function).

Proposition 1: For any level set f^l, one can obtain a set $\mathcal{A}^l\subset V$ such that the gradient norms (8) are

$$\begin{aligned}\|(\nabla_w^+ f^l)(u)\|_p &= \Big[\sum_{v\sim u, v\in\mathcal{A}^l} w_{uv}^{p/2}\Big]^{1/p}\chi_{(\partial^+\mathcal{A}^l)}(u) \text{ and}\\ \|(\nabla_w^- f^l)(u)\|_p &= \Big[\sum_{v\sim u, v\notin\mathcal{A}^l} w_{uv}^{p/2}\Big]^{1/p}\chi_{(\partial^-\mathcal{A}^l)}(u)\ \ ,\end{aligned} \tag{11}$$

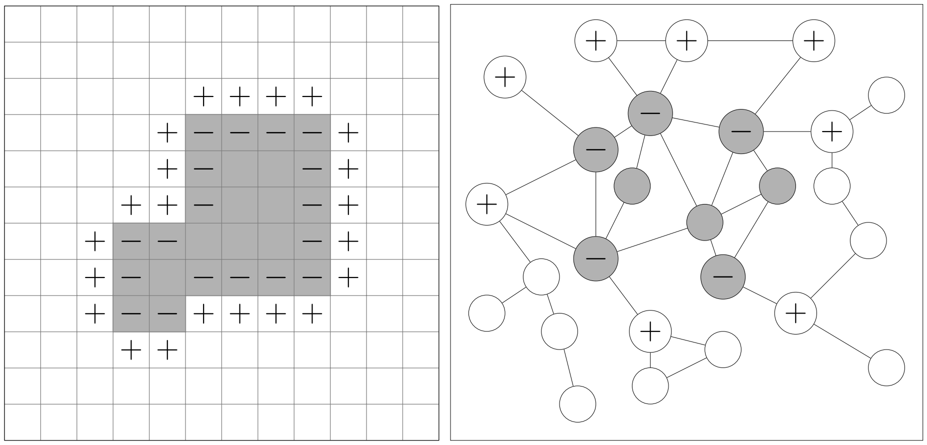

(a) 4-adjacency grid graph (b) Arbitrary graph

Fig. 1. Graph boundary sets on two different graphs. *Gray vertices* correspond to set $\mathcal{A}$. *Plus* and *minus* vertices are external $\partial^+\mathcal{A}$ and internal $\partial^-\mathcal{A}$ sets, respectively.

where $\chi{:}V{\to}\{0,1\}$ is the indicator function and $\mathcal{A}^l$ is the set such that $f^l{=}\chi_{(\mathcal{A}^l)}$.

Proof:

We prove the first relation in (11). One has

$$\|(\nabla_w^+ f^l)(u)\|_p \overset{f^l=\chi_{(\mathcal{A}^l)}}{=} \|(\nabla_w^+ \chi_{(\mathcal{A}^l)})(u)\|_p \overset{(8)}{=} \Big[\sum_{v\sim u} w_{uv}^{p/2} |\max\big(0, \chi_{(\mathcal{A}^l)}(v) - \chi_{(\mathcal{A}^l)}(u)\big)|^p\Big]^{1/p} .$$

We study the cases where $u{\in}\mathcal{A}^l$, $u{\notin}\mathcal{A}^l$ and similarly with its neighborhood $N(u)$.

The only case where $\chi_{(\mathcal{A}^l)}(v){-}\chi_{(\mathcal{A}^l)}(u){>}0$ is when $u{\notin}\mathcal{A}^l$ and its neighbors $v{\in}\mathcal{A}^l$. This configuration corresponds to the definition of the external set of vertices $\partial^+\mathcal{A}^l$ defined in (10). With this property the following relation is deduced:

$$\|(\nabla_w^+ f^l)(u)\|_p = \Big[\sum_{v\sim u, v\in\mathcal{A}^l} w_{uv}^{p/2}\Big]^{1/p} \chi_{(\partial^+\mathcal{A}^l)}(u)$$

Second relation in (11) is obtained with the same scheme: $\chi_{(\mathcal{A}^l)}(v){-}\chi_{(\mathcal{A}^l)}(u){<}0$ only by considering the internal set $\partial^- A^l$ (i.e. $u{\in}A^l$ and $v{\notin}A^l$ with $v{\in}N(u)$). ■

Directly from Proposition (1), the following proposition can be established.

Proposition 2: For any level set f^l, at vertex $u{\in}V$, the $\mathcal{L}_p$-norm of the gradient $(\nabla_w f^l)(u)$ can be decomposed as

$$\|(\nabla_w f^l)(u)\|_p^p{=}\|(\nabla_w^+ f^l)(u)\|_p^p{+}\|(\nabla_w^- f^l)(u)\|_p^p \ .$$

Proof: Using Proposition (1) and the boundary sets $\partial^+\mathcal{A}^l$ and $\partial^-\mathcal{A}^l$, one has

$$\begin{aligned}\|(\nabla_w f^l)(u)\|_p^p &= \sum_{v\sim u} w_{uv}^{p/2}(\alpha_{uv}^l)^p\\ &= \sum_{\substack{v\sim u,\\ u\in\partial^+\mathcal{A}^l}} w_{uv}^{p/2}(\alpha_{uv}^l)^p + \sum_{\substack{v\sim u,\\ u\in\partial^- A^k}} w_{uv}^{p/2}(\alpha_{uv}^l)^p\\ &\overset{\text{Proposition (1)}}{=} \|\nabla_w^+ f^l(u)\|_p^p + \|\nabla_w^- f^l(u)\|_p^p\end{aligned}$$

where $\alpha_{uv}^l = |\chi_{(A^l)}(v) - \chi_{(A^l)}(u)|$. Moreover, we can also deduce that

$$\|(\nabla_w f^l)(u)\|_p = \begin{cases}\|(\nabla_w^+ f^l)(u)\|_p \text{ if } u\in\partial^+\mathcal{A}^l,\\ \|(\nabla_w^- f^l)(u)\|_p \text{ if } u\in\partial^-\mathcal{A}^l.\end{cases}$$

■

Remark 1: Propositions (1) and (2), only consider the $\mathcal{L}_p$-norms where $0<p<+\infty$. For the $\mathcal{L}_\infty$-norm one can demonstrate and obtain same results by using expressions (9).

V. Mathematical morphology by partial difference equations over graphs

In this Section, we present a novel formulation of MM expressed with PDEs-based definitions. First, we introduce our PdEs-based dilation and erosion formulations. Second, we focus on a particular class of morphological filters, the levelings. Finally, based on our morphological framework, we consider the eikonal equation and derive a solution of this equation.

A. PdEs-based dilation and erosion

Starting from PDEs-based dilation and erosion formulations (1), we define the discrete analogue of such definitions and obtain the following expressions with PdEs over graphs. For a given initial function $f^0\in\mathcal{H}(V)$:

$$\begin{aligned}\frac{\partial\delta(f)(u)}{\partial t} &= \partial_t f(u) = +\|(\nabla_w^+ f)(u)\|_p \quad \text{and}\\ \frac{\partial\varepsilon(f)(u)}{\partial t} &= \partial_t f(u) = -\|(\nabla_w^- f)(u)\|_p \quad \forall u\in V\ ,\end{aligned} \tag{12}$$

with the initial condition $\partial_{t=0} f = f^0$ (f is a modified version of f^0) and ∇_w^+ and ∇_w^- are the weighted discrete morphological gradients defined in (7).

To establish (12) we use the decomposition of f into its level sets $f^l = \chi(f-l)$ and the definition of graph boundary sets.

1) Dilation and erosion processes: As for the continuous case, a simple variational definition of dilation applied to f^l can be interpreted as maximizing a surface gain proportional to the gradient norm $+\|\nabla_w f^l\|_p$. Similarly, erosion can be viewed as minimizing a surface gain proportional to $-\|\nabla_w f^l\|_p$.

With Propositions (1) and (2) dilation of f^l on $\mathcal{A}^l$ corresponds to only consider the external boundary set $\partial^+\mathcal{A}^l$ and can be expressed by $\partial_t f^l(u) = +\|(\nabla_w^+ f^l)(u)\|_p$ where the gradient $\|(\nabla_w f^l)(u)\|_p$ is reduced to the external gradient $\|(\nabla_w^+ f^l)(u)\|_p$. Similarly, erosion of f^l on $\mathcal{A}^l$ can be defined by $\partial_t f^l(u) = -\|(\nabla_w^- f^l)(u)\|_p$.

Finally, by extending these two processes for all the levels of f, we can naturally consider the following two families of dilation and erosion. These two processes are parameterized by p and w over any weighted graph $G{=}(V,E,w)$:

$$\delta(f)(u){=}\partial_t f(u){=}+\|(\nabla_w^+ f)(u)\|_p \text{ and} \tag{13}$$

$$\varepsilon(f)(u){=}\partial_t f(u){=}-\|(\nabla_w^- f)(u)\|_p \ . \tag{14}$$

To solve these dilation and erosion processes (13) and (14), on the contrary to the PDEs case, no spatial discretization is needed thanks to derivatives that are directly expressed in a discrete form. Then, by using discretization in time, and with the usual notation $f(u,n){\approx}f(u,n\Delta t)$, the general iterative scheme for dilation and erosion, can be defined at time $n{+}1$, for all $u \in V$, as

$$f^{n+1}(u){=}f^n(u){+}\Delta t\|(\nabla_w^+ f)^n(u)\|_p \text{ and} \tag{15}$$

$$f^{n+1}(u){=}f^n(u){-}\Delta t\|(\nabla_w^- f)^n(u)\|_p \ . \tag{16}$$

The initial condition is $f^{(0)}{=}f^0$ where $f^0{\in}\mathcal{H}(V)$ is the initial function defined on the graph vertices.

If dilation is considered and with the corresponding gradient norms, (15) becomes for $0{<}p{<}{+}\infty$

$$f^{n+1}(u) \overset{(8)}{=} f^n(u){+}\Delta t\Big(\sum_{v\sim u} w_{uv}^{p/2}\big|\max\big(0,\beta_{uv}^n\big)\big|^p\Big)^{\frac{1}{p}} \tag{17}$$

and for $p{=}\infty$

$$f^{n+1}(u) \overset{(9)}{=} f^n(u){+}\Delta t \max_{v\sim u}\Big(w_{uv}^{1/2}\big|\max\big(0,\beta_{uv}^n\big)\big|\Big) \ , \tag{18}$$

where $\beta_{uv}^n{=}f^n(v){-}f^n(u)$.

At each step of the algorithms, the new value at vertex u only depends on its value at step n and the existing values in its neighborhood.

Remark 2: In the case of a vector valued function $f : V \to \mathbb{R}^m$ with $f(u){=}(f_i(u))_{i=1,\ldots,m}$ for all $u{\in}V$, morphological processing is performed on each component f_i independently, leading to m morphological processes. Component wise processing can have drawbacks. To overcome this limitation, morphological processes acting on vector-valued function need to take into account the inner correlation between vector-valued functions. In our methodology, the edges' weight function acts as a coupling term between these components that enables to overcome this limitation.

2) Related schemes in image processing: Dilation (15) and erosion (16) formulations operate on any graph structures. In the sequel, we show that with an adapted graph topology and an appropriated weight function, the proposed methodology for dilation and erosion is linked to well-known methods defined in the context of image processing.

Osher-Sethian discretization scheme. Let $G_0{=}(V,E,g_0)$ be an unweighted 4-adjacency grid graph associated with a grayscale image defined as function $f^0{:}V{\subset}\mathbb{Z}^2{\to}\mathbb{R}$, (17) recovers the exact Osher-Sethian [10] upwind first order discretization scheme of dilation . For $p{=}2$ and G_0, (17) becomes

$$f^{n+1}(u){=}f^n(u){+}\Delta t\Big[\sum_{v\sim u}|\max\big(0,f^n(v){-}f^n(u)\big)\big|^2\Big]^{\frac{1}{2}} \quad . \tag{19}$$

By replacing vertices $u{\in}V$ and their neighborhoods $N(u)$ by their spatial image coordinates (x,y), (19) can be rewritten as

$$\begin{aligned} f^{n+1}((x,y)){=}&f^n((x,y))\\ &+\Delta t\Big[|\min\big(0,f^n((x,y)){-}f^n((x{-}1,y))\big)\big|^2\\ &+|\max\big(0,f^n((x{+}1,y)){-}f^n((x,y))\big)\big|^2\\ &+|\min\big(0,f^n((x,y)){-}f^n((x,y{-}1))\big)\big|^2\\ &+|\max\big(0,f^n((x,y{+}1)){-}f^n((x,y))\big)\big|^2\Big]^{1/2} \end{aligned}$$

since $\max(0,a{-}b)^2{=}\min(0,b{-}a)^2$. Same property can be demonstrated for the erosion case.

Algebraic formulation. The proposed dilation expression also recovers the classical algebraic flat morphological dilation formulation over graphs. In the case where $p{=}\infty$ with a constant discretization time $\Delta t{=}1$ and a constant weight function g_0, (18) becomes for $u{\in}V$:

$$f^{n+1}(u){=}f^n(u){+}\max_{v\sim u}\Big(\max\big(0,\beta^n_{uv}\big)\Big) \quad . \tag{20}$$

Then,

$$f^{n+1}(u){=}\begin{cases} f^n(u){+}\max\limits_{v\sim u}\big(f^n(v)\big){-}f^n(u) \text{ if } \beta^n_{uv}>0 \ , \\ f^n(u) \text{ otherwise} \quad . \end{cases}$$

For both cases, (20) recovers the algebraic dilation over graphs.

$$f^{n+1}(u){=}\max_{v\sim u}\big(f^n(v),f^n(u)\big) \quad . \tag{21}$$

In that case, the structuring element is provided by both the graph topology and the vertices' neighborhoods. For instance, if we consider a 8-adjacency image grid graph, it is equivalent to a dilation by a square structuring element of size $3{\times}3$.

One can demonstrate the same result for the erosion case, where the latter can be defined as

$$f^{n+1}(u){=}\min_{v\sim u}\big(f^n(v),f^n(u)\big) \quad . \tag{22}$$

It is important to note that for the case of weighted graphs, the proposed morphological operators are operators that adapt their behavior according to the importance of weights with their neighbors.

B. Levelings on weighted graphs

Maragos and Meyer [27] have introduced nonlinear PDEs that model a general class of morphological filters: the levelings. Particular cases of such filters are reconstruction openings and closings.

Using the proposed methodology, we define the discrete analogue of continuous morphological levelings over graphs by PdEs. For $u \in V$, leveling processes can be defined as

$$\partial_t f(u) = \mathrm{sgn}(f^0(u) - f(u)) \|(\nabla_w^{\pm} f)(u)\|_p \tag{23}$$

with the initial condition $f = m$ at $t = 0$. Reference function is $f^0 \in \mathcal{H}(V)$ and marker function is $m \in \mathcal{H}(V)$ from which a reconstruction can be produced. $\mathrm{sgn}(x)$ is the sign function with $\mathrm{sgn}(x)$ equals 1 if $x > 0$, -1 if $x < 0$ and 0 if $x = 0$.

Equation (23) is a sign-varying process where $\mathrm{sgn}(f^0 - f)$ controls the evolution and stops when $f^0 = f$. If $f^0 > f$ then (23) acts as dilation and process (13) is recovered where $\nabla_w^{\pm} = \nabla_w^{+}$. If $f^0 < f$ then (23) acts as erosion and process (14) is recovered where $\nabla_w^{\pm} = \nabla_w^{-}$. Finally, at convergence of (23), the leveling of f^0 is obtained with respect to the marker function m.

Equation (23) is defined on weighted graphs of arbitrary structure and provides a novel approach of morphological levelings. The same scheme operates on any discrete data that can be represented by a weighted graph.

Remark 3: Let $G_0 = (V, E, g_0)$ be an unweighted 4-adjacency grid graph associated with a grayscale image. In the case where $p = 2$, with dilation and erosion algorithms presented in previous Section, (23) recovers the exact numerical scheme proposed by [27] to solve PDEs-based levelings.

C. Eikonal equation over weighted graphs

In this Section, we propose an adaptation of the eikonal equation on weighted graphs [29].

The applications of eikonal equation are numerous in image analysis and computer vision such as shape-from-shading [37]–[39], image segmentation [40]–[42] or geodesic distance computation on discrete and parametric surfaces [43]–[47].

The eikonal equation is a particular case of the following general continuous Hamilton-Jacobi equation:

$$\begin{cases} H(x, f, \nabla f) = 0 & x \in \Omega \subset \mathbb{R}^n \\ f(x) = \phi(x) & x \in \Gamma \subset \Omega \end{cases} \tag{24}$$

where ϕ is a positive speed function defined on Ω and Γ represents the sources. The eikonal equation can be expressed by using the following Hamiltonian:

$$H(x, f, \nabla f) = \|\nabla f(x)\| - P(x) \ , \tag{25}$$

where $P(x)$ is a given potential function. The solution of (25) represents the weighted shortest distance from x to the zero distance curve given by Γ (where $\phi(x) = 0$).

In literature, usual methods used to solve (24) are based on discretization of the Hamiltonian and leads to nonlinear systems of equations. The latter system is usually solved by iterative [37], Fast Marching [48] or Fast Sweeping [49] methods.

Another approach to solve (25) is to consider a time dependent version of the equation and to evolve it to the steady state. Then, (25) can be rewritten as

$$\begin{cases} \partial f(x,t)/\partial t = -\|\nabla f(x)\| + P(x) & x{\in}\Omega \subset \mathbb{R}^n \\ f(x,t) = \phi(x) & x{\in}\Gamma \subset \mathbb{R}^n \\ f(x,0) = \phi_0(x) & x{\in}\Omega \end{cases} . \tag{26}$$

In this work, we propose an adaption of (26) on weighted graphs.

With the morphological processes described by (14), the time dependent eikonal formulation (26) can be viewed as an erosion process regarding the minus sign and a null potential function P. Then, by using the corresponding internal gradient (∇_w^-) involved in discrete PdEs-based erosion process, (26) can be directly rewritten with weighted graphs. Given a graph $G{=}(V,E,w)$ and a function $f{\in}\mathcal{H}(V)$, we obtain a discrete PdEs-based version of the system (26) parameterized by w and p [29].

$$\begin{cases} \partial f(u,t)/\partial t = -\|\nabla_w^- f(u)\|_p + P(u) & u{\in}V \\ f(u,t){=}\phi(u) & u{\in}V_0 \subset V \\ f(u,0){=}\phi_0(u) & u{\in}V \end{cases} , \tag{27}$$

where V_0 corresponds to the initial seed vertices.

Remark 4: In this work we only focus on the time-marching approach but, in future works, the resolution of stationary version of the eikonal equation will also be considered.

Using the conventional notation $f^n(u){\approx}f(u,n\Delta t)$, the solution of (27) over weighted graphs of arbitrary topology can be solved by the following algorithm:

$$f^{n+1}(u){=}f^n(u) - \Delta t \left(\|\nabla_w^- f^n(u)\|_p{-}P(u)\right) . \tag{28}$$

Convergence (i.e given a fixed number n of iteration or when $\|f^{n+1}{-}f^n\|{<}\epsilon$) of this process is the solution of the eikonal equation (25).

It is important to note that our formulation of eikonal equation works on any graph structure. This implies that our formulation constitutes a simple method to solve the eikonal equation for any discrete regular or irregular domains that can be modeled by a graph.

Remark 5: Let $G{=}(V,E,g_0)$ be an unweighted graph. Then, (28) corresponds to an iterative version of the Dikjstra shortest path algorithm defined on graphs of arbitrary structure. Indeed, in the case where $p{=}\infty$, $\Delta t{=}1$ and with property (22), (28) is rewritten as

$$f^{n+1}(u) = \min_{v\sim u}(f^n(v)) + P(u) , \tag{29}$$

by considering the neighborhood of u as $N(u){\cup}\{u\}$. This equation corresponds to a shortest path algorithm for a given graph where at each step, the distance $f(u)$ at vertex u corresponds to the minimal distance in its neighborhood.

Moreover, with an unweighted 4-adjacency grid graph and $p{=}2$, one can remark that (28) recovers the Osher-Sethian Hamiltonian discretization scheme [10].

VI. Experiments in image processing

In this Section, experiments are presented to show potentialities and behaviors of our formulation in order to process images. The objective of the following results is not to solve a particular application. Moreover, in this Section, we focus on the case of images and use the natural grid representation of such data. The case of arbitrary graphs will be discussed in the next Section.

In the sequel, morphological operations such as dilation, closing and levelings are presented. Moreover, results for nonlocal image segmentation and weighted distances computation based on our solution of eikonal equation are also provided.

A. Adaptative grayscale image morphological operations

In this experiment, we illustrate our graph-based framework through basic morphological operations such as dilation and closing. For a given function $f \in H(V)$, the simplest way to obtain closing operation is to implement it serially as compositions of dilation δ and erosion ε. Then, a closing is $\varepsilon(\delta(f))$.

Figure 2 presents dilation and closing of an original scalar grayscale image (at top of Fig. 2) considered as a function $f^0 : V \subset \mathbb{Z}^2 \to \mathbb{R}$ that defines a mapping from vertices to grayscale pixel values. This example shows the adaptative aspect of our morphological framework. Indeed, proposed results are obtained for different p values, weight functions w, graph topologies G and feature vector F.

First row of Fig. 2 shows results for the case where $p{=}\infty$, $\Delta t{=}1$. This corresponds to the algebraic processing. In that case, the graph structure (a G_2 graph with the city-block distance) and the vertices' neighborhoods provide an equivalent to a circle structuring element of radius equals to 2. The last three next rows show results for the case where $p{=}2$. Second row of Fig. 2 presents results for an unweighted ($w{=}g_0$) 4-adjacency grid graph. This case corresponds to PDEs-based morphological processing. Difference between second and third column is that in the latter case, we use a weighted ($w{=}g_1$) graph instead of an unweighted one. These results show the benefits of weights that enable to better preserve edge information as compared to the unweighted cases. Fourth column presents nonlocal patch-based results. In this example the graph is a 25-adjacency grid graph (a G_2 graph with the Chebyshev distance) weighted by function g_1 associated with patches of size $5{\times}5$ as pixel features. These results clearly show that this morphological processing better preserves image components such as edges, fine structures and repetitive elements. One can also note in that case, the filtering effects in image background and woman face.

B. Nonlocal levelings for textured images

Figure 3 presents the application of levelings (23) in order to process textured images. This example compares the classical approach with our nonlocal patch based method.

First row of Fig. 3 shows original images corrupted with Gaussian noise of standard deviation of 20. Second row presents image markers from which the levelings are performed. These markers are simply obtained by Gaussian filtering. The two last rows show local and nonlocal patch-based results, respectively. Local levelings correspond to classical PDEs-based methods where the corresponding graph is an unweighted 4-adjacency grid graph. Nonlocal

Fig. 2. Adaptative morphological image processing with different p values, weight functions w, graph topologies G, and feature vector F. At top: original image. First and second columns: dilation and closing operations, respectively. First row: algebraic case (p=∞, Δt=1), second row: PDEs case (p=2), third row: weighted case (w=$g1$), fourth row: nonlocal patch-based case (G_2, F_2).

patch-based levelings results are obtained with a 4-adjacency grid graph weighted by g_1 function. This latter graph is coupled with an unweighted 4-NNG$_2$ where the nearest neighbors are obtained in a $5{\times}5$ search window. Edge weights are computed with patches of size $7{\times}7$. Results clearly show superior behaviors of nonlocal processing in order to reconstruct fine and repetitive structures as compare to local one.

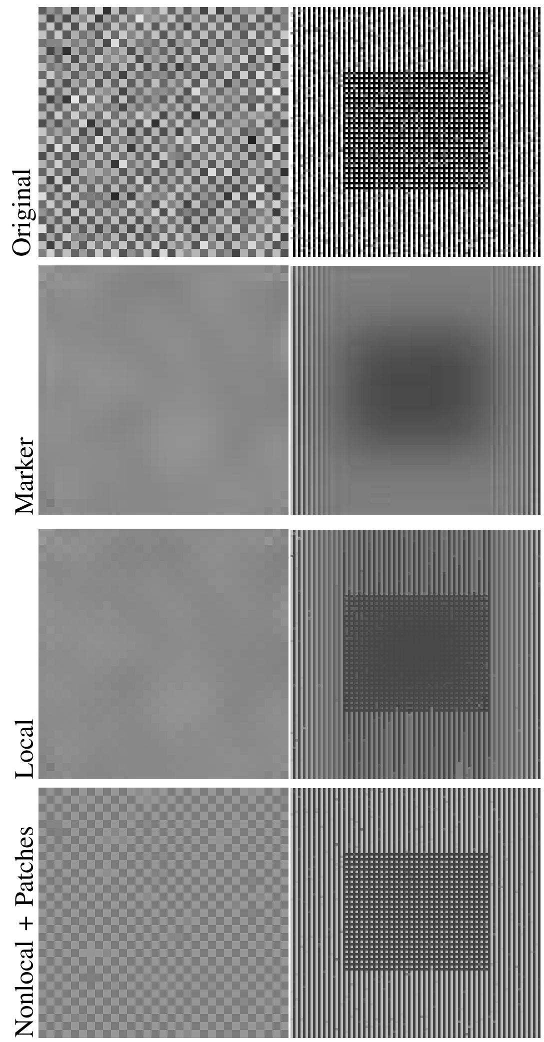

Fig. 3. Textured image levelings: local and nonlocal patch-based processing. First row: noisy original synthetic images. Second row: initial markers obtained by Gaussian filtering. Third row: local approach with G_0, $w{=}g_0$ and $F{=}f^0$. Last row: nonlocal patch-based approach with graph $(G_0, w{=}g_1) \cup (4\text{-NNG}_2, w{=}g_0)$ and features $F{=}F_3(f^0, .)$.

C. Adaptative weighted distances with eikonal equation

Figure 4 shows the application of eikonal equation (28) in order to compute weighted distances. This example shows the adaptivity of our framework. Indeed, results are obtained with different graph topologies, weight functions and p values. Potential function P involved in (28) is equal to 1 and the initial seed is located at the top left corner of the original image.

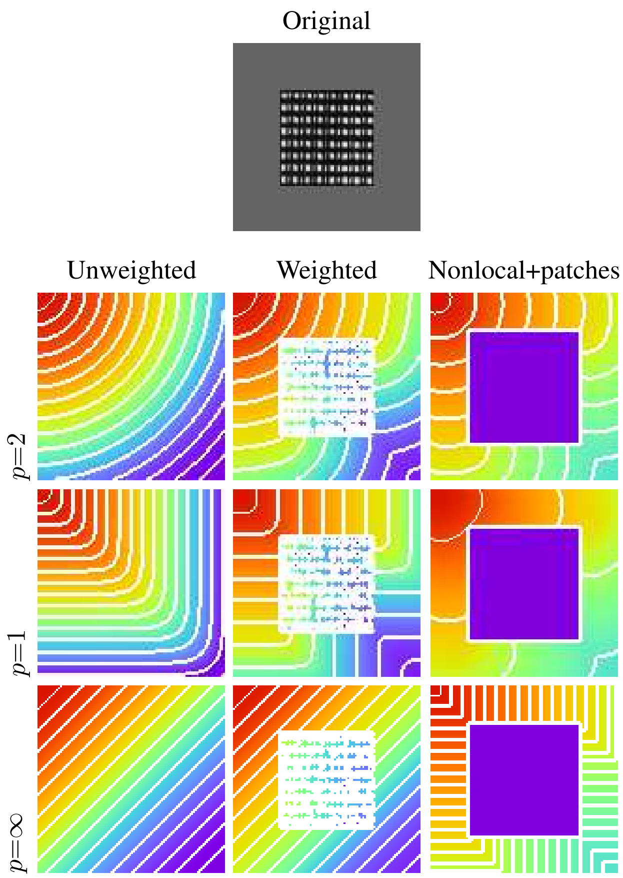

Fig. 4. Adaptative weighted distances computation with different p values, weight functions w and graph topologies G. Results represent color distance maps with iso-level sets. The initial seed is located at the top left corner. At top: original image. First, second and third rows: results with $p{=}2, 1$ and ∞ respectively. First, second and third columns, the graph configurations are: $G_0, w{=}g_0, F{=}f^0$; $G_0, w{=}g_1, F{=}f^0$ and $G_2, w{=}g_1, F{=}F_5(f^0, .)$, respectively

First, second and third rows of Fig. 4 show results for $p{=}2, 1$ and ∞, respectively. All results correspond to color distance maps (red color for small and blue color for large distances) where iso-levels sets are superimposed in white. First column shows results obtained with an unweighted 4-adjacency grid graph that correspond to the classical distances computation. Results in the second column are obtained with the same graph but weighted. With non constant weights, image information is automatically integrated in the distance computation that modifies the front evolution speed particularly into the textured sub-image. Last column shows the nonlocal patch-based case where the graph G_2 is constructed with the Chebyshev distance and weighted by function g_1 associated with patches of size $11{\times}11$. In this case, repetitive information are naturally captured by the weights that stops the front evolution around the textured sub-image. Finally, one can obtain a segmentation of the textured sub-image simply by thresholding the obtained distance maps.

D. Nonlocal interactive image segmentation with eikonal equation

The previous Section has shown applications of our formulation of eikonal equation in order to compute weighted distances. Computed distance maps can be used to perform image segmentation simply by using a threshold or a class membership probability.

In this Section, we propose to address image interactive segmentation problem. Interactive segmentation can be viewed as a semi-supervised graph clustering formulated as follows. Let $G{=}(V,E,w)$ be a weighted graph representing the data to cluster. The semi-supervised vertices clustering consists in grouping the set V into k classes where the number of k classes is given. V is composed of *labeled* and *unlabeled* data. Let $V_0{=}\{u_i\}_{i=1,\dots,k}$ be the set of initial labeled vertices and let $V\backslash V_0$ be the initial unlabeled vertices. The objective is to estimate the unlabeled data from labeled ones. To address this problem, methods based on regularization on graphs have been proposed so far (see [50] and references therein).

In this paper, we propose to consider this clustering problem by using the resolution of eikonal equation (28) and to compute k distance maps where the set V_0 corresponds to initial seeds. At the end of these processes, class membership probabilities can be estimated and the final classification obtained for a given vertex $u{\in}V$ by the following formulation:

$$\underset{i}{\operatorname{argmin}}\{f_i(u)/\sum_i f_i(u)\} \text{ with } i{\in}1,\dots,k \ . \tag{30}$$

Figure 5 shows examples of semi-supervised graph clustering applied to nonlocal interactive image segmentation. The first column shows the original images with user initial seeds superimposed. The red seeds correspond to the object to segment and the green ones correspond to image background. In this example, the eikonal equation is solved by using non constant potential function: the original image gradient. The three last columns of this figure, show segmentation results where white boundaries correspond to the boundaries of segmented regions found by class membership (30) at convergence. These results also show the behavior of our method for different graph topologies and weight functions. The second column of Fig. 5 shows results corresponding to classical methods. The third column shows a weighted case. One can note that weights enable to better capture edge information. Last column shows nonlocal patch-based image segmentations. These results clearly demonstrate the benefits of such graph configurations especially for textured and noisy image, where classical methods fail to found correctly the desired object.

VII. Extension to arbitrary discrete data and graphs

The proposed morphological framework works on graphs of arbitrary topology. One of the advantages is that any discrete data set that can be represented by a weighted graph can be processed with our methodology. As a result, our formulation provides a natural extension of PDEs-based method to any discrete data even if they are defined in high dimensional or irregular domains. In the sequel, through different experiments, morphological processing and applications of eikonal equation for unorganized multivariate data sets are provided. To process vector-valued functions, the scheme described at the end of Sect. V-A1 is applied.

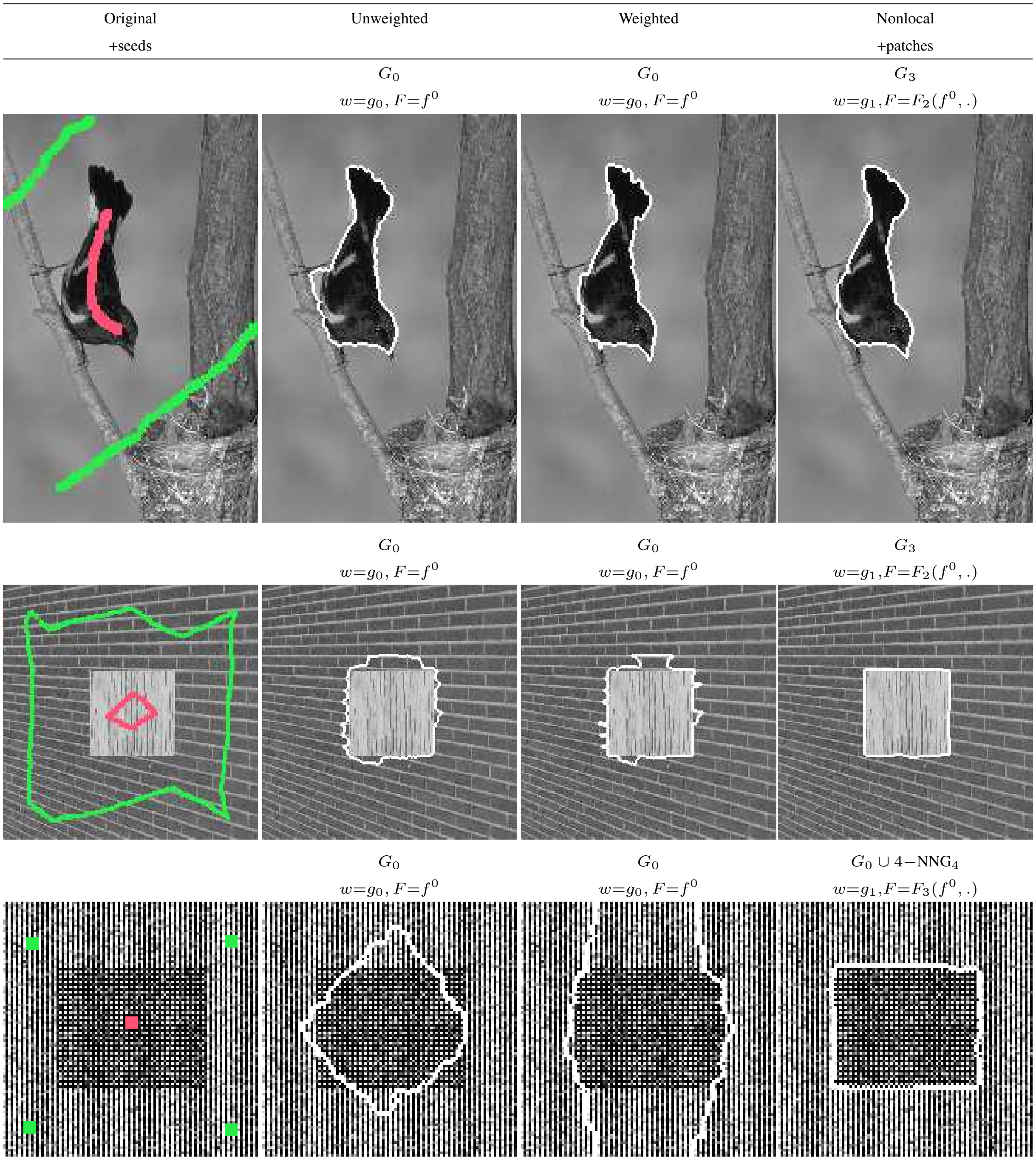

Fig. 5. Interactive image segmentation by eikonal equation with different graph topologies and weight functions. First column: original images with user initial seeds superimposed. Second, third and fourth columns: boundaries of segmented regions superimposed on original images with the specified graph topology G, weight function w and image features F.

A. Data sets alternated sequential filtering

Figure 6 shows application of morphological alternated sequential filters on data sets. An alternated sequential filter consists in an iterative filtering that alternate opening and closing operations.

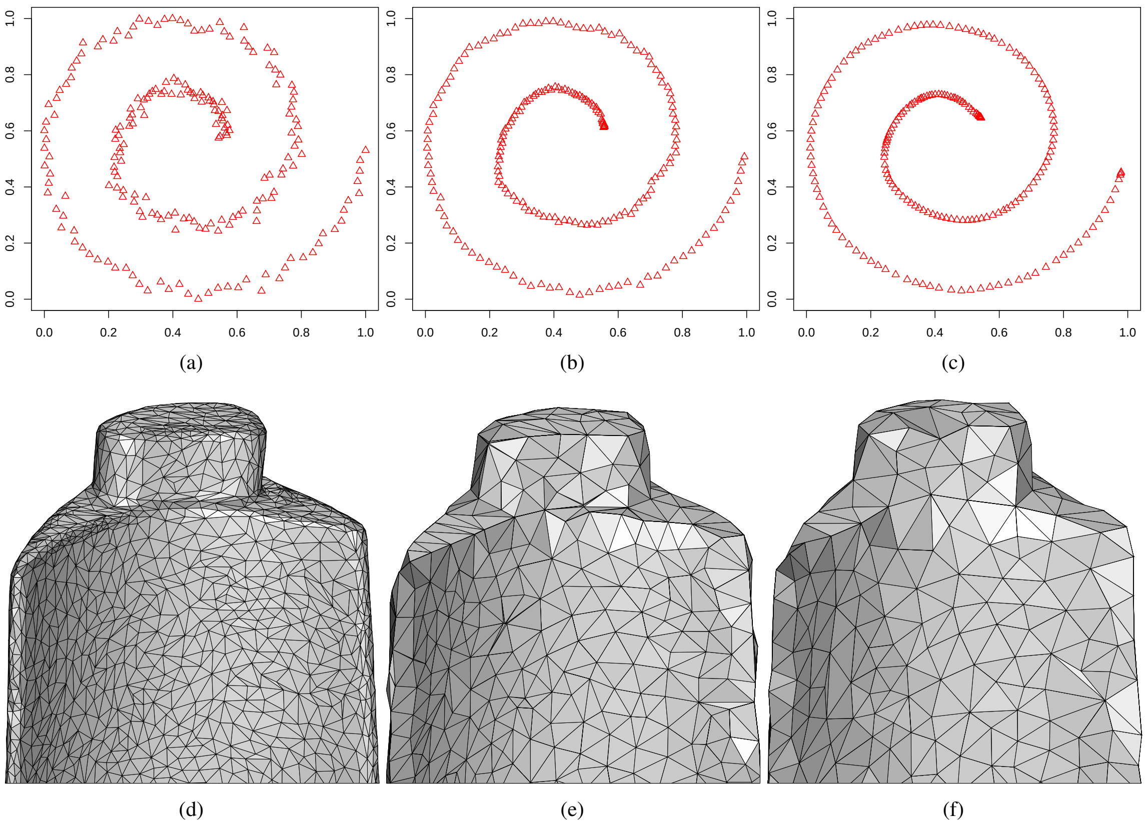

Fig. 6. Data sets alternated sequential filtering. (a) noisy original data, (b) and (c) filtering results for iterations n=2 and n=4 respectively. These results are obtained with a 10-NNG with weight function g_1. (d) original mesh, (e) and (f) filtering results for iteration n=10 and n=50 respectively. These results are obtained with weight function g_1.

First row of Fig. 6 shows the denoising effect of alternated sequential filters on a noisy data set (Fig. 6(a)) that initially represents a spiral. The graph associated to this raw data corresponds to a 10-NNG weighted by function g_1 where each vertex is associated to the spatial coordinates of the corresponding data point. Figures 6(b) and 6(c) show denoising results at iterations n=2 and n=4, respectively. One can appreciate the denoising effect that finally recovers a satisfying spiral shape.

Second row of Fig. 6 shows the simplification effect of alternated sequential filtering on 3D data (mesh). Fig. 6(d) shows a zoomed part of a mesh. The graph corresponds here to the natural graph representation of meshes where each vertex is associated to the 3D spatial coordinates of each mesh point. This latter graph is weighted by function g_1. Figures 6(e) and 6(f) show the evolution of the simplification for iterations n=10 and n=50, respectively. It is important to note that the number of vertices does not change during the filtering process and vertices have moved to similar spatial coordinates.

B. Morphological processing of unorganized high dimensional data sets

Figure 7 shows examples of real world databases processing within our morphological framework.

The first row of this figure shows the original data sets. For the digits case, images come from the United States Postal Service (USPS) handwritten database. This database consists in grayscale images scanned from digits 0 to 9. Each image is of size 16×16. For the head poses case, the original database consists in 133 grayscale images of size 29×29. In these experiments, we use three randomly subsampled test sets of 100 samples for each database.

The second row presents the graphs associated with the original data sets: k-NN graphs weighted with function g_2. It is important to note that each vertex of the graphs corresponds to an image sample and is described by a 256-dimensions ($\mathbb{R}^{16\times16}$) feature vector for the digits database and a 841-dimensions ($\mathbb{R}^{29\times29}$) feature vector for the head poses case. Each feature corresponds to a pixel grayscale value.

The third, fourth and fifth rows show dilation, erosion and opening operations, respectively. One can note the filtering and simplification effects of opening operation on the data. Indeed, this operation tends to reduce the data to new artificial and uniform image samples. Finally, such morphological operations on databases can be used as pre-processing steps for classification or clustering methods.

C. Eikonal equation on topological graphs

The proposed formulation of eikonal equation operates on graphs of arbitrary structure. The advantage is that we can easily apply our resolution of the eikonal equation for any data that can be represented by a graph.

Figure 8 shows examples on structured graphs that represents organized 2D and 3D data. These examples illustrate the front propagation on 2D graph (a Delaunay graph) and on a 3D graph (a mesh). Each vertex of the processed graph is defined by the spatial coordinates of the corresponding data point. The first column shows the original graphs where the initial seed is located by a black circle. Graphs are weighted by weight function g_2 in order to take into account vertex coordinates. The three next columns show the front propagation and the corresponding distance map where red color corresponds to small distances and blue color corresponds to large distances. Last column shows the final distance maps obtained at convergence of algorithm (28). These examples illustrate that our methodology for the eikonal equation can be easily used in order to compute distances on any data that can be represented by a graph.

D. Eikonal equation for nonlocal interactive segmentation based on RAG

In this experiment, we show the advantages to change the graph topology in the context of interactive image segmentation. The idea here, is to use other image structures such as image regions instead of image pixels. To this aim, we compute a pre-segmentation of an original image. This partition can be obtained by any methods such as watershed or energy partitions [51]. Figures 9(b) and 9(f) show examples of partitions obtained from original images (Figs. 9(a) and 9(e)). These images show partitions where each pixel value is replaced by its surrounding region mean color value and where regions boundaries are superimposed in white color. Then, one can compute region-based graphs from these partitions such as Region Adjacency Graph (RAG). The graphs used to obtained segmentation results in Fig. 9 are based on a RAG associated with region-based k-NN graphs and weighted by weight

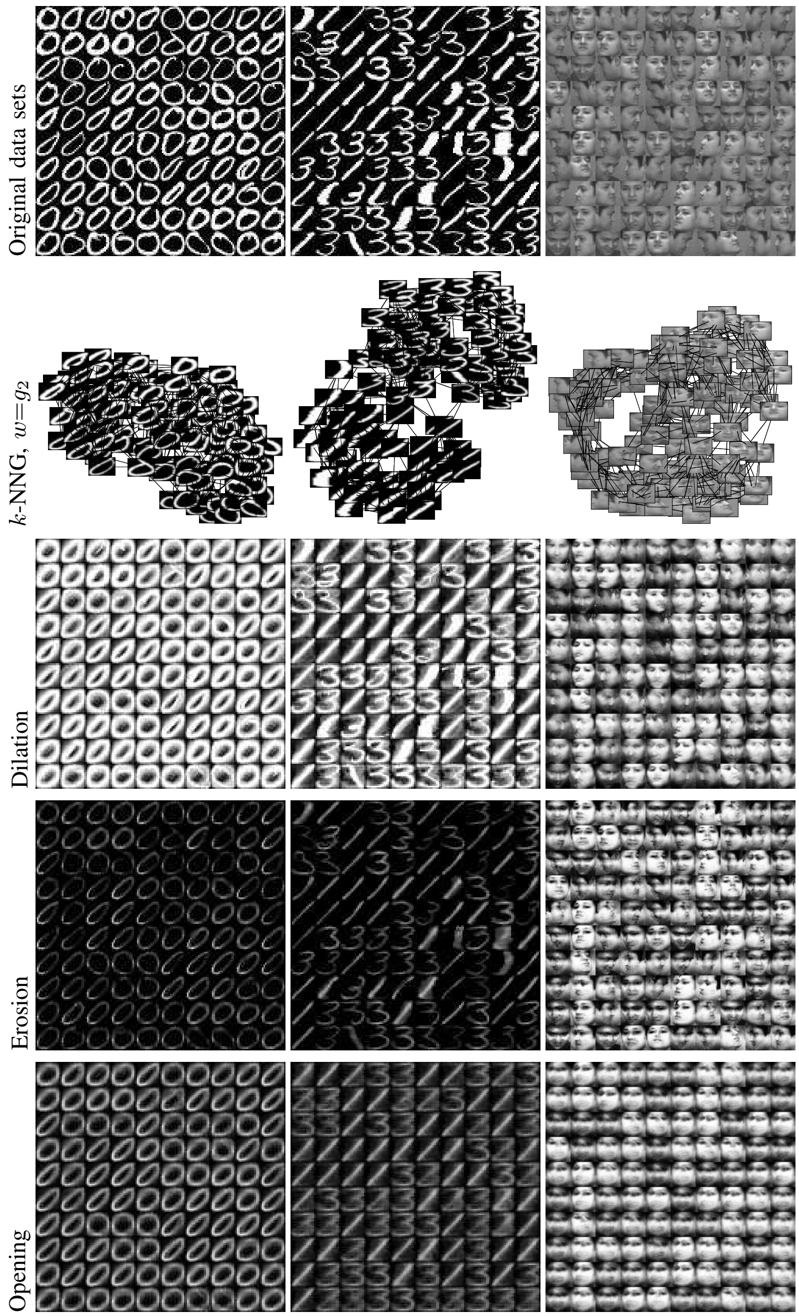

Fig. 7. Morphological processing of high dimensional unorganized data sets. First row: original data where for digits case $f^0 : V \rightarrow \mathbb{R}^{256}$ and for head poses case $f^0 : V \rightarrow \mathbb{R}^{841}$. Second row: k-NN graphs associated with data sets. Third, fourth and fifth rows: dilation, erosion and opening results, respectively.

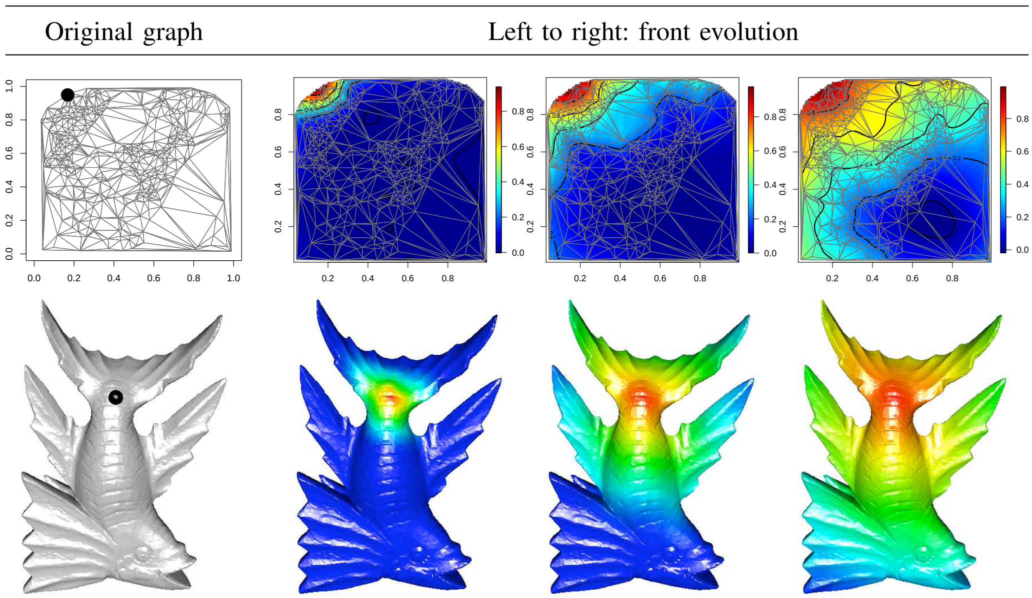

Fig. 8. Front propagation with eikonal equation on topological graphs. First row: 2D graph, second row: mesh. First column: original graphs where the initial seed is located by a black circle. The three last columns: distance evolution where each image corresponds to a distance map where red color represents small distances and blue color large distances. Last column corresponds to final distance map.

function g_1. Results in second and fourth rows of Fig. 9 are obtained with a RAG $\cup$ 1-NNG and a RAG $\cup$ 4-NNG, respectively. Using such graph structure has the following advantages.

- Fast computation. By reducing the number of graph vertices to consider, the computation time is reduced (here 98.5% of reduction in terms of vertices as compared to a pixel-based graph).
- Minimal initial seed. With an appropriate graph structure, the segmentation requires a minimal number of initial user seeds as shown in the second and fourth rows.
- Non local segmentation. The last row of Fig. 9 shows a nonlocal object segmentation, where only one cell is marked and other cells are found by our method even if the objects are not spatially close or even connected.
- Robustness. Figures 9(c), 9(d), 9(g) and 9(h) show the robustness of our method where same results are obtained with different initial seeds position.

VIII. Conclusion

In this paper, a novel formalism of MM operators based on PdEs over weighted graphs of arbitrary topology is proposed. This provides a framework that extends PDEs-based methods to discrete local and nonlocal schemes. Moreover, this enables to process by morphological means any high dimensional unorganized multivariate data. The integration of nonlocal patch-based approach was highlighted for morphological processing as an efficient way to preserve fine and repetitive structures. Within this morphological framework, a discrete version of the eikonal equation over weighted graphs of arbitrary structure is also proposed. The proposed formulation of MM and eikonal equation constitutes a simple, common and adaptative framework that recovers well-known definitions and unifies

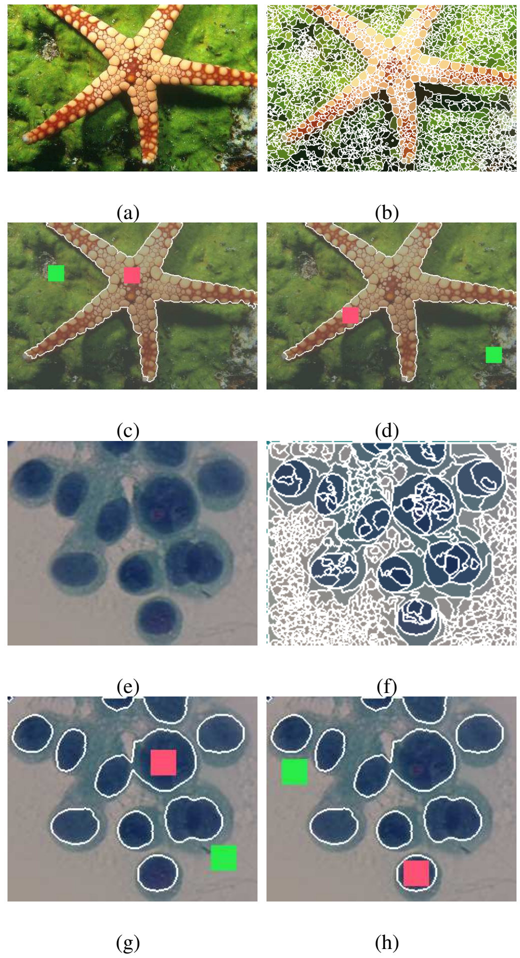

Fig. 9. Interactive segmentation based on RAG. (a) and (e): original images. (b) and (f): image partitions (98.5% of reduction in term of vertices) with mean color and region boundaries superimposed. (c), (d), (g) and (h): segmentation results with segmented region boundaries and initial user seeds.

local and nonlocal configurations in the context of image processing. Through experiments, we have shown the potentiality and the flexibility of our approach to address image morphological processing and image segmentation. Fast processing of images has also been proposed by considering the Region Adjacency Graph instead of the usual grid graph. Finally, we have shown the ability of our methodology to process any unorganized high dimensional data sets that can be useful for data mining, clustering or classification methods.

Acknowledgments

This work was partially supported under a research grant of the ANR Foundation (ANR-06-MDCA-008-01/FO-GRIMMI) and a doctoral grant of the Conseil Régional de Basse-Normandie and of the Cœur et Cancer association in collaboration with the Department of Anatomical and Cytological Pathology from Cotentin Hospital Center.

References

[1] G. Matheron, *Random Sets and Integral Geometry*. New York: Wiley, 1975.

[2] J. Serra, *Image Analysis and Mathematical Morphology*. London: Academic, 1982.

[3] C. Ronse, "Why mathematical mophology needs complete lattices," *Signal Processing*, vol. 21, no. 2, pp. 129–154, 1990.

[4] H. Heijmans, *Morphological Image Operators*. Boston: Academic Press, 1994.

[5] P. Soille, *Morphological Image Analysis, Principles and Applications*, 2nd ed. Springer, 2002.

[6] R. van den Boomgaard and A. Smeulders, "The morphological structure of images: The differential equations of morphological scale-space," *IEEE Trans. Pattern Anal. Mach. Intell.*, vol. 16, no. 11, pp. 1101–1113, 1994.

[7] R. Brockett and P. Maragos, "Evolution equations for continuous-scale morphological filtering," *IEEE Trans. Signal Process.*, vol. 42, no. 12, pp. 3377–3386, 1994.

[8] L. Alvarez, F. Guichard, P.-L. Lions, and J.-M. Morel, "Axioms and fundamental equations of image processing," *Archive for Rational Mechanics and Analysis*, vol. 123, no. 3, pp. 199–257, September 1993.

[9] M. Breuß, B. Burgeth, and J. Weickert, "Anisotropic continuous-scale morphology," in *In Proceedings of the 3rd IbPRIA*, ser. LNCS, J. Martí, Ed., vol. 4478. Springer Berlin / Heidelberg, 2007, pp. 512–522.

[10] S. Osher and J. Sethian, "Fronts propagating with curvature-dependent speed: Algorithms based on Hamilton-Jacobi formulations," *Journal of Computational Physics*, vol. 79, pp. 12–49, 1988.

[11] A. Arehart, L. Vincent, and B. Kimia, "Mathematical morphology: The hamilton-jacobi connection," in *International Conference on Computer Vision*, 1993, pp. 215–219.

[12] G. Sapiro, R. Kimmel, D. Shaked, B. Kimia, and A. Bruckstein, "Implementing continuous-scale morphology by curve evolution," *Pattern Recognition*, vol. 26, no. 9, pp. 1363–1372, 1993.

[13] E. Aptoula and S. Lefèvre, "A comparative study on multivariate mathematical morphology," *Pattern Recognition*, vol. 40, no. 11, pp. 2914–2929, 2007.

[14] J. Angulo, "Unified morphological color processing framework in a lum/sat/hue representation," in *Proc. of ISMM*, 2005, pp. 387–396.

[15] B. Burgeth, A. Bruhn, S. Didas, J. Weickert, and M. Welk, "Morphology for matrix data: Ordering versus pde-based approach," *Image and Vision Computing*, vol. 25, no. 4, pp. 496–511, April 2007.

[16] H. Heijmans, P. Nacken, A. Toet, and L. Vincent, "Graph morphology," *Journal of Visual Communication and Image Representation*, vol. 3, no. 1, pp. 24–38, March 1992.

[17] F. Meyer and R. Lerallut, "Morphological operators for flooding, leveling and filtering images using graphs," in *In Proceedings of the 6th IAPR-TC-15 GbRPR 2007*, ser. LNCS, F. Escolano and M. Vento, Eds., vol. 4538, 2007, pp. 158–167.

[18] J. Postaire, R. Zhang, and C. Lecocq-Botte, "Cluster analysis by binary morphology," *IEEE Trans. Patt. Anal. Machine Intell.*, vol. 15, no. 2, pp. 170–180, February 1993.

[19] A. Buades, B. Coll, and J. Morel, "Nonlocal image and movie denoising," *International Journal of Computer Vision*, vol. 76, no. 2, pp. 123–139, february 2008.

[20] G. Gilboa and S. Osher, "Nonlocal operators with applications to image processing," UCLA, Los Angeles, Report 07-23, July 2007.

[21] G. Peyré, "Image processing with non-local spectral bases," *SIAM Multiscale Modeling and Simulation*, vol. 7, no. 2, pp. 703–730, 2008.

[22] A. Elmoataz, O. Lézoray, and S. Bougleux, "Nonlocal discrete regularization an weighted graphs: a framework for image and manifolds processing," *IEEE Trans. Image Process.*, vol. 17, no. 7, pp. 1047–1060, 2008.

[23] S. Bougleux, A. Elmoataz, and M. Melkemi, "Discrete regularization on weighted graphs for image and mesh filtering," in *Scale Space and Variational Methods in Computer Vision*, ser. LNCS, vol. 4485, 2007, pp. 128–139.

[24] V.-T. Ta, A. Elmoataz, and O. Lézoray, "Partial difference equations over graphs: Morphological processing of arbitrary discrete data," in *Proc. 10th European Conference on Computer Vision (ECCV 2008)*, 2008, accepted for publication.

[25] ——, "Partial difference equations on graphs for mathematical morphology operators overs images and manifolds," in *Proc. 15th International Conference on Image Processing (ICIP 2008)*, 2008, accepted for publication.

[26] A. Elmoataz, O. Lézoray, S. Bougleux, and V.-T. Ta, "Unifying local and nonlocal processing with partial difference operators on weighted graphs," in *International Workshop on Local and Non-Local Approximation in Image Processing (LNLA 2008)*, January 2008, pp. 11–26.

[27] P. Maragos and F. Meyer, "Nonlinear PDEs and numerical algorithms for modeling levelings and reconstruction filters," in *Scale-Space Theories in Computer Vision*, ser. LNCS, vol. 1682, 1999, pp. 363–374.

[28] V.-T. Ta, A. Elmoataz, and O. Lézoray, "Nonlocal morphological levelings by partial difference equations over weighted graphs," in *Proc. 19th International Conference on Pattern Recognition (ICPR 2008)*, 2008, accepted for publication.

[29] ——, "Adaptation of eikonal equation over weighted graphs," in *Proc. 2nd International Conference on Scale Space and Variational Methods in Computer Vision, accepted for publication (SSVM 2009)*, 2009, accepted for publication.

[30] R. Haralick, S. Sternberg, and X. Zhuang, "Image analysis using mathematical morphology," *IEEE Trans. Pattern Anal. Mach. Intell.*, vol. 9, no. 4, pp. 532–550, 1987.

[31] R. Brockett and P. Maragos, "Evolution equations for continuous-scale morphology," in *IEEE International Conference on Acoustics, Speech, and Signal Processing, 1992*, vol. 3, 1992, pp. 125–128.

[32] R. Diestel, *Graph Theory*, 3rd ed., ser. Graduate Texts in Mathematics. Springer-Verlag Heidelberg, 2005, vol. 173.

[33] J. Jaromczyk and G. Toussaint, "Relative neighborhood graphs and their relatives," *Proc. of the IEEE*, vol. 80, no. 9, pp. 1502–1517, 1992.

[34] A. Efros and T. Leung, "Texture synthesis by non-parametric sampling," in *Proc. of the International Conference on Computer Vision (ICCV)*, 1999, pp. 1033–1038.

[35] A. Bensoussan and J.-L. Menaldi, "Difference equations on weighted graphs," *Journal of Convex Analysis*, vol. 12, no. 1, pp. 13–44, 2004.

[36] J.-F. Rivest, P. Soille, and S. Beucher, "Morphological gradients," *Journal of Electronic Imaging*, vol. 2, no. 4, 1993.

[37] E. Rouy and A. Tourin, "A viscosity solutions approach to shape-from-shading," *SIAM J. Num. Anal.*, vol. 29, pp. 867–884, 1992.

[38] J. Sethian, "A fast marching level set methods for monotonically advancing fronts," *Proc. Nat. Acad. Sci.*, vol. 41, no. 2, pp. 199–235, 1999.

[39] E. Prados and O. Faugeras, "Shape from shading," in *The Handbook of Mathematical Models in Computer Vision*, N. Paragios, Y. Chen, and O. Faugeras, Eds. Springer, 2005, pp. 377–390.

[40] L. D. Cohen and R. Kimmel, "Global minimum for active contour models: A minimal path approach," *IJCV*, vol. 24, pp. 57–58, 1997.

[41] P. Maragos and M. Butt, "Curve evolution, differential morphology and distance transforms as applied to multiscale and eikonal problems," *Fundamentae Informatica*, vol. 41, pp. 91–129, 2000.

[42] L. Yatziv, A. Bartesaghi, and G. Sapiro, "A fast O(n) implementation of the fast marching algorithm," *Journal of Computational Physics*, vol. 212, pp. 393–399, 2006.

[43] A. M. Bronstein, M. M. Bronstein, and R. Kimmel, "Weighted distance maps computation on parametric three-dimensional manifolds," *J. Comput. Phys.*, vol. 225, no. 1, pp. 771–784, 2007.

[44] J. A. Sethian and A. Vladimirsky, "Ordered upwind methods for static hamiton-jacabi equations: Theory and algorithms," *SIAM J. Num. Anal.*, vol. 41, no. 1, pp. 325–363, 2003.

[45] R. Abgrall, "Numerical discretization of the first-order hamilton-jacobi equations on triangular meshes," *Comm. Pure and Applied Math.*, vol. 49, pp. 1339–1373, 1996.

[46] Chi-Wang Shu and Yong-Tao Zhang, "High order WENO schemes for hamilton-jacobi equations on triangular meshes," *SIAM J. Scien. Comp.*, vol. 24, pp. 1005–1030, 2003.

[47] F. Mémoli and G. Sapiro, "Fast computation of weighted distance functions and geodesics on implicit hyper-surfaces," *J. Comput. Phys*, vol. 173, pp. 730–764, 2001.

[48] J. A. Sethian, *Level Set Methods and Fast Marching Methods. Evolving Interfaces in Computational Geometry, Fluid Mechanics, Computer Vision, and Materials Science*, 2nd ed. Cambridge University Press, 1999.

[49] H. K. Zhao, "Fast sweeping method for eikonal equations," *Math. Comp.*, vol. 74, pp. 603–627, 2005.

[50] V.-T. Ta, O. Lézoray, A. Elmoataz, and S. Schüpp, "Graph-based tools for microscopic cellular image segmentation," *Pattern Recognition*, vol. 42, no. 6, pp. 1113–1125, jun 2009.

[51] P. Arbeláez and L. Cohen, "Energy partitions and image segmentation," *Journal of Mathematical Imaging and Vision*, vol. 20, no. 1–2, pp. 43–57, 2004.